JOURNAL OF VIROLOGY, Jan. 2004, p. 257–265 Vol. 78, No. 1
0022-538X/04/$08.00+0 DOI: 10.1128/JVI.78.1.257–265.2004

Evidence for an Essential Catalytic Role of the F10 Protein Kinase in Vaccinia Virus Morphogenesis

Patricia Szajner,[1,2] Andrea S. Weisberg,[1] and Bernard Moss[1]*

Laboratory of Viral Diseases, National Institute of Allergy and Infectious Diseases, National Institutes of Health, Bethesda, Maryland 20892,[1] and Graduate Program of the Department of Genetics, The George Washington University, Washington, D.C. 20052[2]

Received 16 July 2003/Accepted 12 September 2003

Temperature-sensitive mutants of vaccinia virus, with genetic changes that map to the open reading frame encoding the F10 protein kinase, exhibit a defect at an early stage of viral morphogenesis. To further study the role of the enzyme, we constructed recombinant vaccinia virus vF10V5i, which expresses inducible V5 epitope-tagged F10 and is dependent on a chemical inducer for plaque formation and replication. In the absence of inducer, viral membrane formation was delayed and crescents and occasional immature forms were detected only late in infection. When the temperature was raised from 37 to 39°C, the block in membrane formation persisted throughout the infection. The increased stringency may be explained by a mild temperature sensitivity of the wild-type F10 kinase, which reduced the activity of the very small amount expressed in the absence of inducer, or by the thermolability of an unphosphorylated kinase substrate or uncomplexed F10-interacting protein. Further analyses demonstrated that tyrosine and threonine phosphorylation of the A17 membrane component was inhibited in the absence of inducer. The phosphorylation defect could be overcome by transfection of plasmids that express wild-type F10, but not by plasmids that express F10 with single amino acid substitutions that abolished catalytic activity. Although the mutated forms of F10 were stable and concentrated in viral factories, only the wild-type protein complemented the assembly and replication defects of vF10V5i in the absence of inducer. These studies provide evidence for an essential catalytic role of the F10 kinase in vaccinia virus morphogenesis.

Vaccinia virus (VV) has a linear double-stranded DNA genome of approximately 190 kbp that encodes nearly 200 proteins involved in transcription, DNA replication, RNA and protein processing, and virus assembly, all of which occur in the cytoplasm (11). The formation of the initial viral membrane represents one of the most interesting and least understood of the events in the poxvirus replication cycle. Electron microscopic studies have provided conflicting models for the origin of the viral membrane (16), and coupled genetic and biochemical investigations are needed to uncover the underlying mechanism. Virus morphogenesis is interrupted at successive or partially overlapping stages when cells are infected with mutants that have genetic changes mapping to the F10L, A17L, D13L, and A14L open reading frames (ORFs). Under nonpermissive conditions, the F10 mutants make no recognizable viral membranes (21, 23), the A17 mutants accumulate vesicles and tubules (13, 14, 25), the D13 mutants make irregular membrane sheets (26), and the A14 mutants accumulate vesicles and empty crescents (15, 22). Nearly identical phenotypes, characterized by numerous viral crescent membranes that appear normal except for their location at a distance from the viroplasm and accumulation of empty immature virions, occur when expression of A30 (19, 20), G7 (17), or J1 (2) is repressed.

The F10L ORF encodes a protein kinase that is incorporated into virus particles (10) and phosphorylates or regulates the phosphorylation of serine, threonine, and tyrosine residues of the A17 and A14 membrane components (1, 4, 22). Taken together, the data suggest a role for the F10 kinase in morphogenesis that is mediated at least in part by phosphorylation of A17. Nevertheless, there has been no study demonstrating that the role of F10 in assembly is dependent on its catalytic activity. The need for such experiments is underscored by our recent finding that F10 is part of a complex that contains several other proteins that are likely to have structural roles in assembly (18). In addition, the data supporting the role of the F10 kinase in membrane formation have been derived solely from temperature-sensitive (*ts*) mutants. Although *ts* mutants have provided valuable insights into the mechanisms employed in various stages of the VV replication cycle, the phenotype can be distorted because of interactions of improperly folded proteins or secondary effects due to the higher than normal temperature. This is especially true for protein kinases, since the defect at the nonpermissive temperature could be derived from the thermolability of an unphosphorylated acceptor protein, in addition to that of the kinase itself, as has been proposed for the VV B1 protein kinase by Rempel and Traktman (12). It can be helpful, therefore, to characterize additional types of conditional lethal mutants. Here we describe the construction and assembly defect of a conditional lethal VV mutant in which expression of F10 is repressed in the absence of a specific inducer. We used the mutant in transcomplementation assays to demonstrate that point mutations of conserved kinase domains in F10 abolished catalytic activity and prevented phosphorylation of A17 and virus morphogenesis.

* Corresponding author. Mailing address: Laboratory of Viral Diseases, National Institutes of Health, 4 Center Dr., MSC 0445, Bethesda, MD 20892-0445. Phone: (301) 496-9869. Fax: (301) 480-1147. E-mail: bmoss@nih.gov.

MATERIALS AND METHODS

ORF designations. ORFs are designated by a capital letter indicating a *Hin*dIII restriction endonuclease fragment, a number indicating the position in the *Hin*dIII fragment, and a letter (L or R) indicating the direction of transcription, e.g., F10L. The corresponding protein is designated by a capital letter and number, e.g., F10.

Cells and viruses. VV (WR strain) and the recombinant virus vT7LacOI (24) were propagated in HeLa cells as previously described (6). The newly constructed vF10V5i was propagated in the presence of 50 μM isopropyl-β-D-thiogalactopyranoside (IPTG) and 2.5% fetal bovine serum. Plaque assays were performed on BS-C-1 cell monolayers in six-well tissue culture plates with 0.5% methylcellulose as described previously (7).

Antibodies. Antiserum against a peptide corresponding to amino acids 5 to 20 of F10 followed by a cysteine residue (NDSSPEYQWMSPHRLSC) was produced in rabbits (Covance Research Products, Denver, Pa). Anti-A14, anti-H3, and anti-A17N antisera were used as previously described (1, 3). The murine monoclonal antibody (MAb) MHA.11 (Covance) recognizes the 9-amino-acid influenza virus hemagglutinin (HA) epitope tag and the murine MAb anti-V5 (Invitrogen, Carlsbad, Calif.) recognizes the 14-amino-acid sequence found in the P and V proteins of the paramyxovirus simian virus 5. Rabbit polyclonal anti-phosphotyrosine (anti-pTyr) and anti-phosphothreonine (anti-pThr) antisera were purchased from Zymed Laboratories (South San Francisco, Calif.).

Western blot analysis. Proteins from infected cell lysates or purified virions were resolved by sodium dodecyl sulfate-polyacrylamide gel electrophoresis (SDS-PAGE), electrophoretically transferred to a nitrocellulose membrane, blocked overnight with either 10% nonfat dried milk or 5% bovine serum albumin, and probed with rabbit polyclonal antibody or mouse MAb followed by anti-rabbit or anti-mouse immunoglobulin G conjugated to horseradish peroxidase, essentially as described previously (20). Bound immunoglobulin G was detected with the SuperSignal West Pico chemiluminescent substrate (Pierce, Rockford, Ill.).

Plasmid and recombinant virus construction. The pVOTE.2F10V5 plasmid, containing the F10L ORF modified by silent mutations and a V5 tag at the C terminus flanked by *Nde*I and *Sac*II restriction sites at the 5′ and 3′ ends, respectively, was constructed by standard PCR methods and inserted into pVOTE.2 (24). The F10 knockout plasmid contained (i) a complete copy of the ORF encoding the enhanced green fluorescent protein (GFP) under the control of the VV F10 promoter and (ii) flanking sequences of the F10L ORF comprising a portion of the F11L ORF (right flank) and a complete copy of the F9L ORF plus a portion of the F8L ORF (left flank). The pP11F10HA-WT plasmid, containing a copy of the F10L ORF under the control of the VV P11 promoter and modified by silent point mutations and by an HA tag at the C terminus, was constructed by standard PCR methods. The plasmids containing mutated copies of the F10L ORF under the control of the P11 promoter and a C-terminal HA tag, namely pP11-F10$_{G96D}$HA, pP11-F10$_{D307A}$HA, and pP11-F10$_{D343A}$HA, were constructed by use of the QuikChange site-directed mutagenesis kit according to the instructions of the manufacturer (Stratagene, La Jolla, Calif.). The pP11F10HA-WT plasmid was used as a template for all reactions.

Recombinant VV vF10/F10V5i was constructed from vT7LacOI (24) and pVOTE.2F10V5 by homologous recombination, using previously described procedures (7). vF10/F10V5i was then used to generate vF10V5i by recombination with the F10 knockout plasmid. Fluorescent plaques containing the recombinant virus expressing GFP were picked and used to infect fresh monolayers of BS-C-1 cells three successive times to isolate vF10V5i.

In vitro protein kinase assay. Approximately 3×10^7 BS-C-1 cells were infected with vF10V5i at a multiplicity of infection of 3 in the absence of IPTG and either mock transfected or transfected with 15 μg of plasmid. Twenty-four hours after infection, the cells were harvested, washed with ice-cold phosphate-buffered saline (PBS), and lysed with a mixture containing 10 mM Tris (pH 7.5), 150 mM NaCl, 0.5% (vol/vol) Triton X-100, 0.2% (wt/vol) deoxycholic acid, and protease inhibitor cocktail tablets (Roche Molecular Biochemicals, Indianapolis, Ind.) for 30 min on ice. Lysates were clarified by centrifugation at 20,000 × *g* for 30 min at 4°C and then cleared with 50 μl of 20% protein A-Sepharose beads for 1 h at 4°C. The cleared lysate was then centrifuged at 100 × *g* for 1 min and the supernatant was incubated with 100 μl of 50% (vol/vol) slurry of the anti-HA affinity matrix (Roche Molecular Biochemicals) for 3 h. The resin was washed four times with lysis buffer and twice with kinase buffer (50 mM Tris [pH 7.5], 20 mM β-glycerophosphate, 5 mM $MgCl_2$, 1 mM dithiothreitol, 1 mM sodium fluoride, 100 μM sodium orthovanadate, and protease inhibitor cocktail tablet). The protein kinase assays were performed in a 30-μl solution containing 20 μl of HA resin bound to F10, 1 μg of dephosphorylated α-casein (Sigma), and 20 mM [γ-^{32}P]ATP in kinase buffer. Reactions were incubated at 30°C for 10 min and were terminated by the addition of SDS-PAGE sample buffer.

RESULTS

Construction of a conditionally lethal inducible F10 mutant. A mutant VV, with a modified F10 gene that is regulated by IPTG, was constructed by homologous recombination. We started with recombinant vT7LacOI (24), containing (i) the bacteriophage T7 RNA polymerase gene regulated by a VV late promoter coupled to the *Escherichia coli lac* operator and (ii) the *E. coli lac* repressor gene expressed continuously by a VV early-late promoter. The first step was the insertion of a V5 epitope-tagged copy of the F10L ORF, regulated by a bacteriophage T7 promoter and *E. coli lac* operator, into the HA locus of vT7LacOI. The resulting intermediate virus, vF10/F10V5i, contained the original F10L ORF as well as the new inducible copy. Next, the original F10L ORF was deleted from vF10/F10V5i by homologous recombination using a plasmid containing the GFP ORF under the control of the F10 promoter, flanked by sequences upstream and downstream of the endogenous F10L ORF. The final recombinant virus, vF10V5i, was plaque purified in the presence of 50 μM IPTG and contained a single IPTG-inducible V5-tagged copy of the F10L ORF.

The presence of two *lac* operators, one regulating expression of the T7 RNA polymerase and the other regulating a V5 epitope-tagged F10V5 gene with a T7 promoter, provided two levels of repression. The formation of vF10V5i plaques was dependent on IPTG (data not shown). In a one-step growth experiment, the yield of vF10V5i increased with IPTG concentrations up to 25 μM and reached a plateau at higher concentrations of IPTG (data not shown). A time course experiment indicated that the kinetics of replication of vF10V5i in the presence of 50 μM IPTG were similar to those of VV WR (Fig. 1A). In contrast, the yield of vF10V5i barely increased over a 48-h period in the absence of IPTG (Fig. 1A). The difference in yields in the presence and absence of IPTG was approximately 2 log.

Repression and induction of F10V5 synthesis. Cell lysates, prepared from BS-C-1 cells infected with vF10V5i in the absence or presence of 50 μM IPTG, were analyzed by SDS-PAGE and Western blotting with anti-V5 MAb. In the presence of IPTG, the expected band of 50 kDa was detected at 6 h and increased progressively in intensity (Fig. 1B). In the absence of IPTG, the 50-kDa F10V5 band was barely detected at 24 h, but not at the earlier time points examined (Fig. 1B), indicating a low basal level of expression also found in other mutants of this type. For comparison, the Western blots were also probed with antibody against the VV protein encoded by the H3L ORF. H3 was expressed equally in the absence or presence of IPTG (Fig. 1B). Under the latter conditions, H3 and F10V5 were synthesized with similar kinetics, although a VV late promoter and a T7 promoter, respectively, regulated them.

The kinetics of F10 synthesis during an infection with wild-type virus were not previously reported, although late expression was predicted from the putative promoter sequences and the presence of early transcriptional termination motifs within the F10L ORF (10). The 50-kDa F10 band was detected by

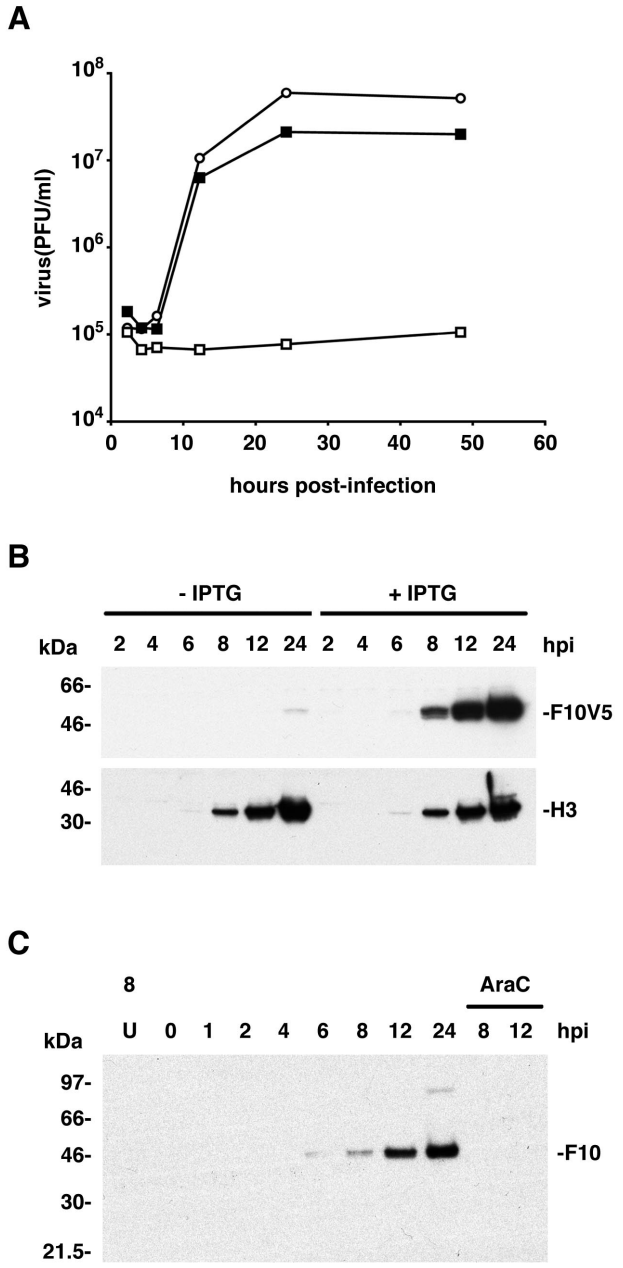

FIG. 1. Effects of IPTG on the replication of vF10V5i and synthesis of the F10 protein. (A) Effect of IPTG on virus yield. BS-C-1 cells were infected with VV WR (○) or vF10V5i in the absence (□) or presence (■) of 50 μM IPTG. Cells were harvested at the indicated times after infection and virus titers were determined by plaque assay in the presence of IPTG. (B) Effect of IPTG on F10V5 and H3 protein synthesis. BS-C-1 cells were infected at a multiplicity of infection of 10 with vF10V5i in the presence or absence of 50 μM IPTG and harvested at intervals between 2 and 24 h postinfection (hpi). Proteins from total cell lysates were resolved by electrophoresis on a 10 to 20% polyacrylamide gradient gel in SDS-Tricine buffer, analyzed by Western blotting using anti-V5 or anti-H3 antibody, and detected by chemiluminescence. The numbers on the left correspond to the molecular masses of marker proteins. The positions of the F10V5 and H3 bands are indicated on the right. (C) Temporal synthesis of F10 in cells infected with WR. BS-C-1 cells were mock infected for 8 h (U) or infected at a multiplicity of infection of 10 in the absence or presence of AraC and harvested between 0 and 24 h postinfection (hpi). Proteins from whole-cell extracts were analyzed by Western blotting as in panel A except that the antiserum was prepared against a peptide composed of amino acids 5 to 20 of F10.

Western blotting 6 h after infection and continued to increase in intensity during the remainder of the 24-h time course (Fig. 1C), similar to the kinetics of induced F10 expression (Fig. 1B). F10 was not detected in lysates of cells infected with VV in the presence of cytosine arabinoside (AraC) (Fig. 1C), demonstrating that the F10 promoter has no early component. An additional Western blotting experiment showed that the amount of F10 made by vF10V5i in 50 μM IPTG was a little higher than that made by wild-type VV (data not shown).

Taken together, these data indicated that the block in vF10V5i replication can be attributed to inhibition of F10 expression in the absence of IPTG, while the kinetics of F10 expression and virus replication are similar to those of wild-type virus in the presence of IPTG.

Morphogenesis of vF10V5i under nonpermissive conditions. Several of the major core proteins undergo proteolytic cleavage by a process that is coupled to morphogenesis and can be prevented by the drug rifampin (9). Pulse-chase experiments were performed to determine whether repression of F10 expression affected the proteolytic processing of viral proteins. Pulse-chase experiments revealed that processing of the P4a and P4b precursors was inhibited to similar extents in cells infected with vF10V5i in the absence of IPTG or with WR in the presence of rifampin (data not shown). A similar inhibition occurs during infections with F10 *ts* mutants at the nonpermissive temperature (21, 23). These results suggested that morphogenesis of VV particles was blocked in cells infected with vF10V5i in the absence of IPTG.

To examine morphogenesis directly, cells were infected with vF10V5i in the presence or absence of IPTG and thin sections were examined by electron microscopy. In the presence of IPTG, the replication cycle appeared normal, with numerous membrane crescents and immature virions in nearly all cell sections 8 and 12 h after infection and large numbers of mature virions 24 h after infection (not shown). Eight hours after infection in the absence of IPTG, viral factory regions recognizable by their distinct electron density and exclusion of cellular organelles were present in most thin sections (Fig. 2A), but membrane crescents were very few in number and were detected in only 8 of 50 cell sections examined. Twelve (Fig. 2B) and 24 (Fig. 2C) h after infection without IPTG, the number of sections with crescents increased to 23 and 32 of 50, respectively, but there were still no mature virions.

Eight hours after infection, the appearance of cells infected with vF10V5i in the absence of IPTG resembled that of cells infected with the most stringent F10 *ts* mutants at the nonpermissive temperature (21, 23). At 12 and 24 h, however, the cells infected with vF10V5i in the absence of IPTG resembled those infected with leaky *ts* mutants. We had previously found that an inducible A30 mutant virus more closely resembled a corresponding *ts* mutant at 39°C than at 37°C (19). Experiments were carried out to determine if the phenotype of vF10V5i was temperature dependent. Accordingly, cells were infected with vF10V5i at either 37 or 39°C in the absence of IPTG. Crescent membranes were detected at 24 h in cells infected at 37°C, whereas at 39°C crescents were rare and large dense masses accumulated in areas that were devoid of cellular organelles (Fig. 2D). All stages of virion morphogenesis, including crescents, IV, intracellular mature virions, and intracellular envel-

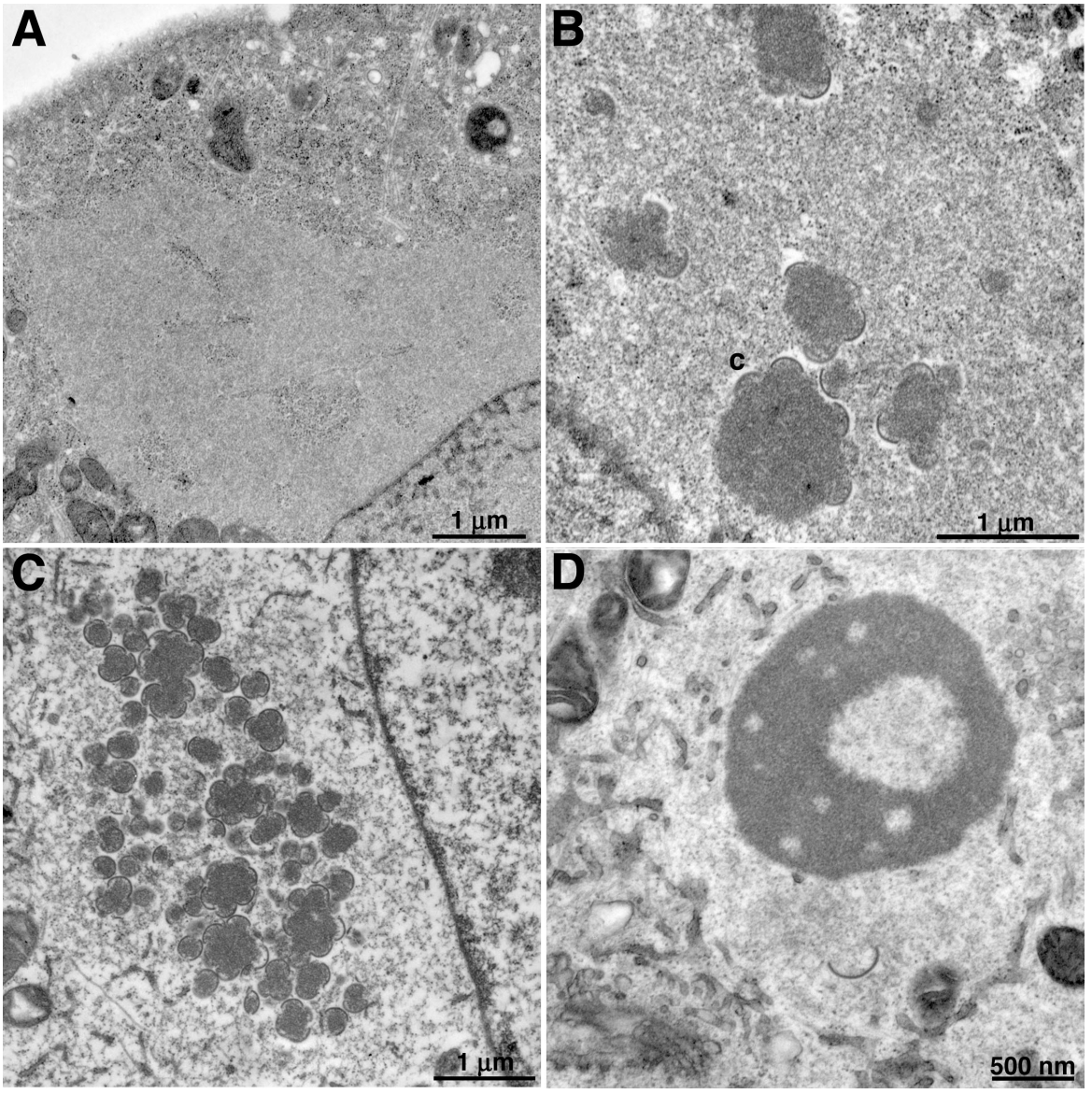

FIG. 2. Electron microscopy of cells infected with vF10V5i. BS-C-1 cells were infected with vF10V5i at a multiplicity of infection of 10 at 37°C (A, B, C) or 39°C (D) in the absence of IPTG. Eight (A), 12 (B), or 24 (C and D) h after infection, the cells were fixed and prepared for transmission electron microscopy essentially as described previously (20). Electron micrographs are shown, with the scales indicated by bars. Abbreviations: C, crescents; nu, nucleoid within an IV.

oped virions, were observed in cells infected at 39°C with the vF10V5i virus in the presence of IPTG (data not shown).

There was a difference in the stability of the F10 protein at 39°C when it was synthesized by the stringent *ts*28 mutant or vF10V5i. Western blotting experiments indicated that 24 h after infection in the absence of IPTG, the amount of F10 was slightly reduced at 39°C compared to 37°C, whereas the amount of F10 was increased at the higher temperature in the presence of IPTG (data not shown). F10 expressed by the stringent F10 *ts*28 mutant, however, was unstable at the elevated temperature, as it was detected by Western blotting at 37°C but not at 39°C (data not shown).

Dependence of A17 phosphorylation and processing on induction of F10 expression. Phosphorylation of the A17 and A14 membrane components fails to occur when cells are infected with the F10 *ts*28 mutant at the nonpermissive temperature (1, 4), as can now be understood by the instability of the mutated protein at 39°C. To determine whether repression of F10 expression has a similar effect at 37°C, immunoblotting experiments were performed with pTyr and pThr antibodies, which recognize tyrosine- and threonine-phosphorylated A17, respectively. The identity of the A17 band was confirmed by using an inducible A17 mutant of VV (25) and antibodies specific to A17 (1). Both tyrosine and threonine phosphorylation of A17 was severely inhibited in the absence of IPTG (Fig. 3, rows 2 and 3), although very weak signals could be detected when the blots were overdeveloped (not shown). The levels of phosphorylated A17 increased proportionally to the concen-

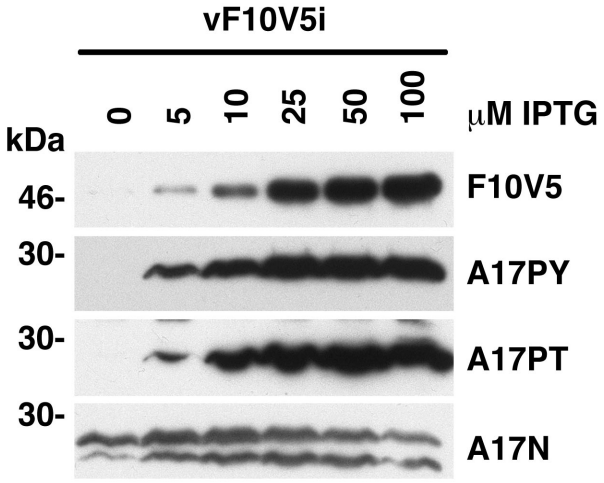

FIG. 3. Effect of IPTG on the synthesis of F10V5 and on the posttranslational modification of A17. BS-C-1 cells were infected with vF10V5i in the presence of 0 to 100 μM IPTG. Twenty-four hours after infection, the cells were harvested and the proteins were analyzed by electrophoresis on a 4 to 20% polyacrylamide gradient gel in SDS-Tris-glycine buffer. The proteins were then transferred to a nitrocellulose membrane and incubated with the anti-V5 (F10V5), anti-pTyr (A17PY), anti-pThr (A17PT), or anti-A17N antibody. The bands were detected by chemiluminescence. The numbers on the left correspond to the molecular masses of the marker proteins.

tration of IPTG and corresponded to the induction of V5-tagged F10 (Fig. 3, row 1). The severe reduction in tyrosine phosphorylation in the absence of IPTG was confirmed by SDS-PAGE analysis of ^{32}P-labeled proteins that bound to pTyr antibody (data not shown).

The repression of F10 had little effect on the amount of A17 protein made, as determined by Western blotting with an antiserum against A17 which recognizes both the phosphorylated precursor and the dephosphorylated C-terminally cleaved forms of A17 (Fig. 3, row 4). Most of the A17 protein detected in cells infected in the absence of IPTG, however, migrated with the precursor form, and only small amounts corresponded to the faster migrating C-terminally cleaved form. In the presence of inducer, however, the proportion of cleaved A17 increased. In addition, the lower band appeared to migrate progressively faster in the cells infected in the presence of increasing amounts of IPTG, suggesting that the cleaved A17 undergoes further modifications during VV infection.

Mutations in the putative active site of F10 abolish kinase activity and phosphorylation of A17. Lin and Broyles (10) recognized several protein kinase motifs in the F10L ORF, including domain I, containing a cluster of glycine residues near the N terminus; domain II, containing the putative active site lysine; and domains VI and VII, with highly conserved aspartic acid residues. The motifs in the F10 kinase, however, had not been tested for their role in catalysis either in vitro or in vivo. We constructed VV late promoter expression plasmids containing the wild-type F10L ORF (pF10HA-WT) and F10L ORFs with the following individual codon mutations: (i) Gly at position 96 to Asp (pP11-F10$_{G96D}$HA), (ii) Asp at position 307 to Ala (pP11-F10$_{D307A}$HA), and (iii) Asp at position 343 to Ala (pP11-F10$_{D343A}$HA). A nonconservative substitution was made in domain I in order to disrupt the local structure, which is thought to be involved in ATP binding. However, the Asp-to-Ala substitutions in domains VI and VII were designed to have minimal effects on structure. The influenza HA tag was added to the C termini of the wild-type and mutated forms of F10 to allow their isolation by affinity purification and detection by Western blotting. Cells were infected with vF10V5i in the absence of IPTG, to repress expression of virus-encoded F10, and transfected with plasmids expressing the HA epitope-tagged F10 regulated by a VV late promoter or a control plasmid. The cells were harvested 24 h after infection and extracts were prepared and incubated with a MAb against the HA tag followed by protein A-agarose beads, which were then extensively washed to remove loosely bound proteins. Western blotting indicated that wild-type and mutated proteins had been successfully isolated by this procedure (Fig. 4A). The washed beads containing bound F10 were incubated with casein and [γ-^{32}P]ATP, and the products were analyzed by SDS-PAGE and autoradiography. An intensely labeled casein band was detected only in the lane containing the product of wild-type F10 (Fig. 4A). These data were in accord with predictions regarding the active site of the F10 kinase.

Next, we carried out experiments to determine whether inactivation of the catalytic activity of the F10 kinase would prevent tyrosine phosphorylation of A17 in infected cells. Following an infection and transfection protocol similar to that used in the above experiment, the whole-cell lysates were analyzed by SDS-PAGE followed by Western blotting with anti-HA MAb to detect F10HA or anti-pTyr antibody to detect phosphorylated A17. The mutated forms of F10 were expressed at higher levels than was wild-type F10 (Fig. 4B), suggesting that inactivation of the kinase site stabilizes the protein. The tyrosine-phosphorylated A17 protein was detected in cells that had been infected with vF10V5i in the absence of IPTG and transfected with the plasmid encoding wild-type F10 and in cells infected with the virus in the presence of IPTG (Fig. 4B). In contrast, when IPTG was omitted, only faint phosphorylated A17 bands were detected for cells transfected with the control vector (mock) or expressing a mutated F10 (Fig. 4B), providing evidence that the catalytic activity of the F10 kinase is required for phosphorylation of A17. Interestingly, the mutated forms of F10 appeared to decrease the background level of A17 phosphorylation, suggesting that they may exert dominant-negative effects.

Wild-type and mutated forms of F10 localize in viral factories. Inactivation of the catalytic site is a likely explanation for the failure of mutated forms of F10 to induce phosphorylation of A17. However, because F10 could also have nonenzymatic roles, we considered the possibility that the mutations caused aberrant intracellular targeting of F10. Because the intracellular localization of F10 was not previously described, we first used the V5 MAb to locate epitope-tagged F10 expressed by vF10V5i in the presence of IPTG. The MAb stained the DNA-containing viral factories in the cytoplasm 8 h (Fig. 5, row 1) as well as 12 and 16 h (not shown) after infection. There was also a hazy reticular staining that could be due to overexpression of V5-tagged F10. Viral factory localization also occurred when HA-tagged wild-type F10 was expressed from a transfected plasmid in cells infected with vF10V5i in the absence of IPTG (Fig. 5, row 2). Furthermore, the same pattern was obtained when each F10 with a point mutation in the kinase motif was

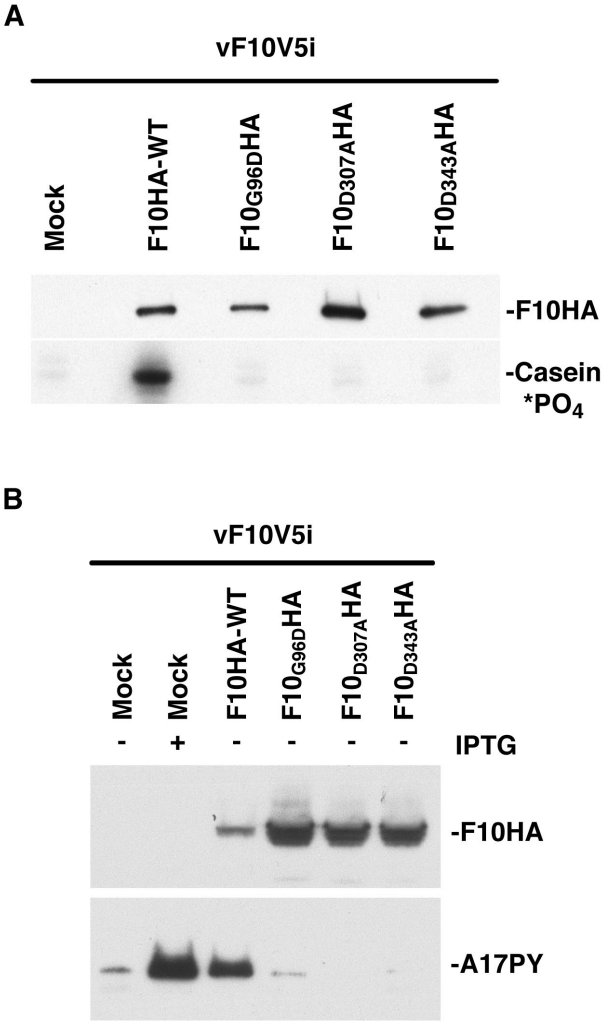

FIG. 4. In vitro and in vivo activity of mutated F10 kinase. (A) In vitro activity. BS-C-1 cells were infected with vF10V5i in the absence of IPTG and either mock transfected or transfected with expression plasmids encoding HA epitope-tagged wild-type F10 (F10HA-WT) or mutated F10 ($F10_{G96D}HA$, $F10_{D307A}HA$, and $F10_{D343A}HA$). Twenty-four hours after infection, the cells were harvested and the wild-type and mutated forms of F10 were bound to an anti-HA affinity matrix. The bound proteins were analyzed by electrophoresis on a 4 to 20% polyacrylamide gradient gel in SDS-Tris-glycine buffer followed by Western blotting using an anti-HA antibody conjugated to horseradish peroxidase. Kinase assays were performed in kinase buffer, with F10HA proteins still attached to the affinity matrix, 20 μM [γ-^{32}P]ATP, and 1 μg of casein. After incubation for 10 min at 30°C, samples were denatured with SDS and analyzed on a 4 to 20% polyacrylamide gradient gel in SDS-Tris-glycine buffer. Proteins were visualized by autoradiography. (B) BS-C-1 cells were infected with vF10V5i in the presence of 50 μM IPTG or in the absence of IPTG and transfected as for panel A. Twenty-four hours after infection, the cells were harvested and total cell lysates were prepared. The proteins were analyzed by electrophoresis on a 10 to 20% polyacrylamide gradient gel in SDS-Tricine buffer. The proteins were then transferred to a nitrocellulose membrane and incubated with anti-HA and anti-pTyr antibodies to detect F10 and tyrosine-phosphorylated A17, respectively. The bands were detected by chemiluminescence.

expressed (Fig. 5, rows 3 to 5). No background labeling was detected with the anti-V5 or anti-HA antibodies in cells infected with WR (data not shown), indicating that these antibodies specifically recognize the tagged versions of F10.

Since the point mutations did not diminish the stability of F10 or alter its intracellular targeting, we attributed the loss of tyrosine phosphorylation of A17 to the elimination of F10 kinase activity.

Transcomplementation of vF10V5i by wild-type F10 but not by F10 with mutations in the kinase active site. Although we showed that the catalytic activity of the F10 kinase is required for phosphorylation of A17, there was no evidence that such phosphorylation is required for virus assembly. F10 is a virion component and physically interacts with other virion proteins required for virus morphogenesis (18). It was possible, therefore, that F10 protein interactions might be more important for virus replication than the kinase activity. This would not be unprecedented, as the essential role of the VV uracil DNA glycosylase is independent of its enzyme activity (5). Since we showed that specific amino acid substitutions in F10 inactivated the catalytic site, we determined whether these mutated proteins could complement the replication of vF10V5i in the absence of IPTG. Complementation assays were carried out by infecting cells with vF10V5i in the absence of IPTG and transfecting them with plasmids expressing wild-type or mutated F10 proteins or GFP. The cells were harvested 24 h after infection and virus titers were determined by plaque assay in the presence of IPTG. In the absence of IPTG, cells transfected with the wild-type F10 plasmid produced 10 times more virus than cells transfected with the control GFP plasmid (Fig. 6). In contrast, no increase in virus titer was observed in cells transfected with any of the three plasmids expressing mutated forms of F10 (Fig. 6).

We also used electron microscopy to determine whether the catalytically inactive kinase could induce the formation of viral crescents and mature virions. Cells were infected with vF10V5i in the absence of IPTG and transfected with the vector plasmid or a plasmid expressing either wild-type or mutated F10. The cells transfected with the plasmid expressing wild-type F10 contained more crescents at both 8 and 24 h than the cells transfected with the vector alone (data not shown). In addition, some cells contained mature virions, in agreement with the complementation of infectivity. In contrast, the cells transfected with plasmids expressing mutated F10 had fewer crescents than those transfected with the vector plasmid, suggesting dominant-negative inhibition (data not shown).

DISCUSSION

To further investigate the role of the F10 kinase, we constructed vF10V5i, a recombinant VV with an IPTG-inducible F10L ORF fused to a V5 epitope tag. We were concerned about leakiness because inducible mutants of this type have been largely used to study abundant structural proteins rather than enzymes, which are usually needed in only small amounts. In the absence of IPTG, vF10V5i did not form plaques or replicate under one-step growth conditions, although a faint band corresponding to the epitope-tagged F10 could be detected by Western blotting 24 h after infection. Electron microscopic images of infected cell sections confirmed an early

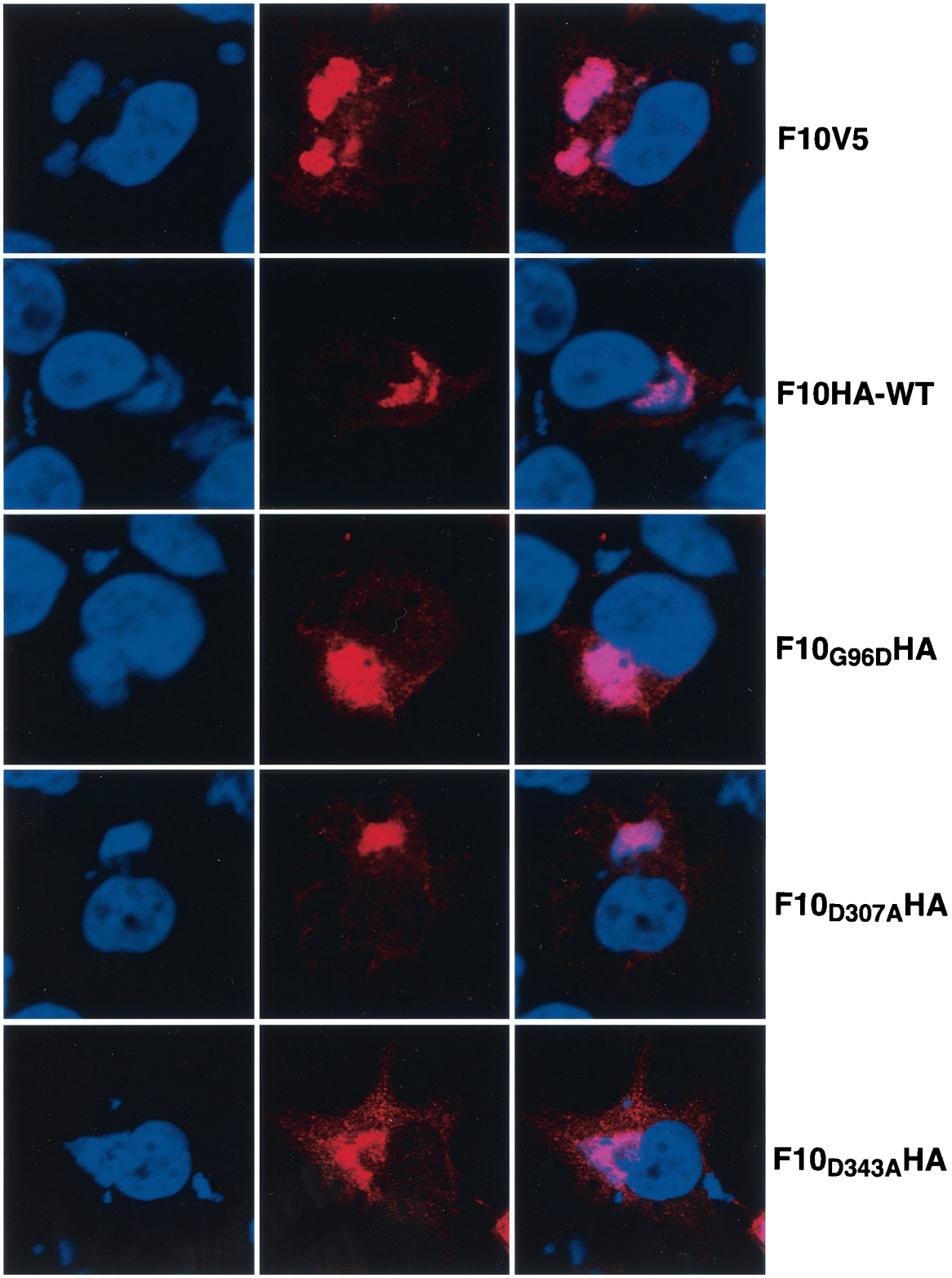

FIG. 5. Localization of F10 by confocal microscopy. HeLa cells were infected with vF10V5i at a multiplicity of infection of 5 in the absence or presence of 25 μM IPTG and transfected with plasmids as described in the legend for Fig. 4. Eight hours after infection, the cells were fixed with 4% paraformaldehyde in PBS for 20 min, washed and permeabilized with 0.1% Triton X-100 in PBS for 7 min, and blocked with 1% bovine serum albumin in PBS for 10 min. The cells infected in the presence of IPTG were stained with the anti-V5 MAb to detect the induced F10V5 protein, while those infected in the absence of the inducer and transfected with plasmids were stained with an anti-HA MAb (column 2). In each case, rhodamine red X-conjugated goat anti-mouse antibody was used as the secondary antibody. DNA in nuclei and viral factories was stained with DAPI (column 1). The cells were examined by confocal microscopy and merged images are shown in column 3. Colors: red, anti-V5 or anti-HA antibody; blue, DAPI.

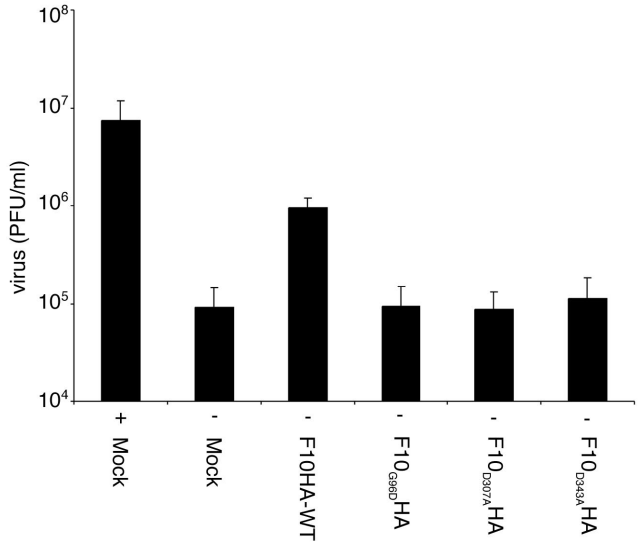

FIG. 6. Transcomplementation of virus infectivity. HeLa cells were infected and transfected as described in the legend for Fig. 4 with (+) or without (−) 50 μM IPTG. After 24 h, the cells were harvested and the virus titers were determined by plaque assay in the presence of 50 μM IPTG. Values are the averages plus standard deviations (error bars) of three independent transfection experiments.

block in virus assembly under nonpermissive conditions. Eight hours after infection in the absence of IPTG, no viral membranes were detected in the cytoplasmic factory areas of the majority of cells examined, whereas in the presence of IPTG there were numerous crescents and circular forms at this time. This difference is highly significant because the permissive and nonpermissive infections were carried out simultaneously and with the same stock of virus, the only difference being the addition of IPTG to one set of cultures and not to the other. We did see some membrane crescents and circular forms in the absence of IPTG at later times, but there was no significant progression to mature virions. One possible explanation for the delay rather than the total elimination of membrane formation is that threshold levels of F10 slowly accumulate in the absence of IPTG. Arrest at the crescent stage could result if unattainable higher threshold levels of F10 were needed for further morphogenesis. Since the F10 kinase may phosphorylate several viral proteins, larger amounts of enzyme might be required for phosphorylation of some acceptors than for others.

Electron microscopic images of cells infected with the most stringent F10 *ts* mutant showed a nearly complete block in viral membrane formation 24 h after infection at the nonpermissive temperature (21, 23). Interestingly, when we infected cells with vF10V5i in the absence of IPTG at 39°C instead of 37°C, we also saw a nearly complete block in viral membrane formation that persisted for 24 h. One explanation is that the wild-type F10 kinase manifests mild temperature sensitivity, which would be sufficient to reduce the activity of the very small amounts of kinase. This temperature sensitivity of the wild-type F10 kinase would have an insignificant biological effect when normal amounts of F10 are produced. This explanation is consistent with the observed thermolability of the purified F10 kinase in vitro (23). Alternatively, an unphosphorylated viral protein or a protein that normally interacts physically with F10 may be thermolabile when F10 is repressed. In this regard, we previously found that elevating the temperature of cells infected with an inducible A30 mutant caused the assembly defect to more closely resemble that of an A30 *ts* mutant at the same temperature (19).

The fact that F10 is a kinase implied that loss of catalytic activity is responsible for the lethality of F10 *ts* mutants at the nonpermissive temperature. The finding that the A17 and A14 membrane components are unphosphorylated at the nonpermissive temperature (1, 4) and the greater in vitro thermolability of a mutated kinase than of the wild type (23) were consistent with this interpretation. Nevertheless, there were no data indicating that phosphorylation of A17 or A14 is essential, and the thermal sensitivity of the mutated kinase could result from a global change in conformation rather than from specific elimination of enzymatic activity. Indeed, we found that F10 made by the *ts*28 mutant was unstable in vivo at the nonpermissive temperature. For this study, we used site-specific mutagenesis to provide more direct evidence for the catalytic role of the F10 kinase in vivo. The catalytic domains of protein kinase family members are not conserved uniformly but consist of alternating regions of high and low conservation (8). Lin and Broyles (10) noted amino acid clusters in the F10L ORF that are characteristic of several protein kinase domains. We made single substitutions of the most highly conserved amino acids of recognizable domains I, VI, and VII and found that they inactivated the kinase activity when assayed in vitro. When expressed by transfection in cells infected with vF10V5i in the absence of IPTG, the mutated proteins were stable and colocalized with the DNA-containing cytoplasmic factories. However, A17 was not tyrosine phosphorylated when any of the mutated forms of F10 were expressed. Moreover, the wild-type F10 but none of the catalytically inactive mutants was able to complement the membrane assembly defect of vF10V5i in the absence of IPTG. Since the F10 kinase phosphorylates multiple viral proteins, further dissection of the system may require the mutagenesis of the phosphate acceptor sites of individual viral proteins.

ACKNOWLEDGMENTS

We thank Eugene Koonin for advice regarding mutagenesis of F10, Brian Ward and Owen Schwartz for assistance in confocal microscopy, and Norman Cooper for providing tissue culture cells.

REFERENCES

1. **Betakova, T., E. J. Wolffe, and B. Moss.** 1999. Regulation of vaccinia virus morphogenesis: phosphorylation of the A14L and A17L membrane proteins and C-terminal truncation of the A17L protein are dependent on the F10L protein kinase. J. Virol. **73:**3534–3543.
2. **Chiu, W. L., and W. Chang.** 2002. Vaccinia virus J1R protein: a viral membrane protein that is essential for virion morphogenesis. J. Virol. **76:**9575–9587.
3. **da Fonseca, F. G., A. Weisberg, E. J. Wolffe, and B. Moss.** 2000. Characterization of the vaccinia virus H3L envelope protein: topology and posttranslational membrane insertion via the C-terminal hydrophobic tail. J. Virol. **74:**7508–7517.
4. **Derrien, M., A. Punjabi, R. Khanna, O. Grubisha, and P. Traktman.** 1999. Tyrosine phosphorylation of A17 during vaccinia virus infection: involvement of the H1 phosphatase and the F10 kinase. J. Virol. **73:**7287–7296.
5. **De Silva, F. S., and B. Moss.** 2003. Vaccinia virus uracil DNA glycosylase has an essential role in DNA synthesis that is independent of its glycosylase activity: catalytic site mutations reduce virulence but not virus replication in cultured cells. J. Virol. **77:**159–166.
6. **Earl, P. L., N. Cooper, S. Wyatt, B. Moss, and M. W. Carroll.** 1998. Preparation of cell cultures and vaccinia virus stocks, p. 16.16.1–16.16.3. *In* F. M. Ausubel, R. Brent, R. E. Kingston, D. D. Moore, J. G. Seidman, J. A. Smith,

and K. Struhl (ed.), Current protocols in molecular biology, vol. 2. John Wiley and Sons, New York, N.Y.

7. **Earl, P. L., B. Moss, L. S. Wyatt, and M. W. Carroll.** 1998. Generation of recombinant vaccinia viruses, p. 16.17.1–16.17.19. *In* F. M. Ausubel, R. Brent, R. E. Kingston, D. D. Moore, J. G. Seidman, J. A. Smith, and K. Struhl (ed.), Current protocols in molecular biology, vol. 2. John Wiley and Sons, New York, N.Y.
8. **Hanks, S. K., A. M. Quinn, and T. Hunter.** 1988. The protein kinase family: conserved features and deduced phylogeny of the catalytic domains. Science **241:**42–52.
9. **Katz, E., and B. Moss.** 1970. Formation of a vaccinia virus structural polypeptide from a higher molecular weight precursor: inhibition by rifampicin. Proc. Natl. Acad. Sci. USA **6:**677–684.
10. **Lin, S., and S. S. Broyles.** 1994. Vaccinia protein kinase 2: a second essential serine/threonine protein kinase encoded by vaccinia virus. Proc. Natl. Acad. Sci. USA **91:**7653–7657.
11. **Moss, B.** 2001. *Poxviridae*: the viruses and their replication, p. 2849–2883. *In* D. M. Knipe and P. M. Howley (ed.), Fields virology, 4th ed., vol. 2. Lippincott Williams & Wilkins, Philadelphia, Pa.
12. **Rempel, R. E., and P. Traktman.** 1992. Vaccinia virus-B1 kinase—phenotypic analysis of temperature-sensitive mutants and enzymatic characterization of recombinant proteins. J. Virol. **66:**4413–4426.
13. **Rodríguez, D., M. Esteban, and J. R. Rodríguez.** 1995. Vaccinia virus A17L gene product is essential for an early step in virion morphogenesis. J. Virol. **69:**4640–4648.
14. **Rodriguez, J. R., C. Risco, J. L. Carrascosa, M. Esteban, and D. Rodriguez.** 1997. Characterization of early stages in vaccinia virus membrane biogenesis: implications of the 21-kilodalton protein and a newly identified 15-kilodalton envelope protein. J. Virol. **71:**1821–1833.
15. **Rodriguez, J. R., C. Risco, J. L. Carrascosa, M. Esteban, and D. Rodriguez.** 1998. Vaccinia virus 15-kilodalton (A14L) protein is essential for assembly and attachment of viral crescents to virosomes. J. Virol. **72:**1287–1296.
16. **Sodeik, B., and J. Krijnse-Locker.** 2002. Assembly of vaccinia virus revisited: de novo membrane synthesis or acquisition from the host? Trends Microbiol. **10:**15–24.
17. **Szajner, P., H. Jaffe, A. S. Weisberg, and B. Moss.** 2003. Vaccinia virus G7L protein interacts with the A30L protein and is required for association of viral membranes with dense viroplasm to form immature virions. J. Virol. **77:**3418–3429.
18. **Szajner, P., A. S. Weisberg, and B. Moss.** 2004. Physical and functional interactions between vaccinia virus F10 protein kinase and virion assembly proteins A30 and G7. J. Virol. **78:**266–274.
19. **Szajner, P., A. S. Weisberg, and B. Moss.** 2001. Unique temperature-sensitive defect in vaccinia virus morphogenesis maps to a single nucleotide substitution in the A30L gene. J. Virol. **75:**11222–11226.
20. **Szajner, P., A. S. Weisberg, E. J. Wolffe, and B. Moss.** 2001. Vaccinia virus A30L protein is required for association of viral membranes with dense viroplasm to form immature virions. J. Virol. **75:**5752–5761.
21. **Traktman, P., A. Caligiuri, S. A. Jesty, and U. Sankar.** 1995. Temperature-sensitive mutants with lesions in the vaccinia virus F10 kinase undergo arrest at the earliest stage of morphogenesis. J. Virol. **69:**6581–6587.
22. **Traktman, P., K. Liu, J. DeMasi, R. Rollins, S. Jesty, and B. Unger.** 2000. Elucidating the essential role of the A14 phosphoprotein in vaccinia virus morphogenesis: construction and characterization of a tetracycline-inducible recombinant. J. Virol. **74:**3682–3695.
23. **Wang, S., and S. Shuman.** 1995. Vaccinia virus morphogenesis is blocked by temperature-sensitive mutations in the F10 gene, which encodes protein kinase 2. J. Virol. **69:**6376–6388.
24. **Ward, G. A., C. K. Stover, B. Moss, and T. R. Fuerst.** 1995. Stringent chemical and thermal regulation of recombinant gene expression by vaccinia virus vectors in mammalian cells. Proc. Natl. Acad. Sci. USA **92:**6773–6777.
25. **Wolffe, E. J., D. M. Moore, P. J. Peters, and B. Moss.** 1996. Vaccinia virus A17L open reading frame encodes an essential component of nascent viral membranes that is required to initiate morphogenesis. J. Virol. **70:**2797–2808.
26. **Zhang, Y., and B. Moss.** 1992. Immature viral envelope formation is interrupted at the same stage by lac operator-mediated repression of the vaccinia virus D13L gene and by the drug rifampicin. Virology **187:**643–653.